Waste Rubber Incorporated in the Alkali-Activated Metakaolin's Aluminosilicate Network Enhanced by Microwave Irradiation

Barbara Horvat, Branka Mušič

Slovenian National Building and Civil Engineering Institute, Ljubljana, Slovenia
barbara.horvat@zag.si, branka.music@zag.si

Building materials represent the possibility of prolonging the life of waste materials. The key is to ensure that the products are suitable for their function. So we activated metakaolin with the alkaline Na-silicate solution in the ratio that ensures the prevention of efflorescence and high mechanical strength (Horvat and Ducman, 2019). As the waste material (to be incorporated in the aluminosilicate network (ASN) of the alkali-activated metakaolin) ground waste rubber from electric cables was used in the preselected mass ratios. Its inclusion in products, like paving stones, can reduce stiffness, improve durability, dampen vibrations, and reduce road noise. The mechanical strengths of test samples with rubber present on the active surface or slightly below were higher compared to samples where rubber was encapsulated throughout the volume. Compressive strength was higher when samples were irradiated with low powers of microwaves while irradiation with higher powers led to the foaming of alkali-activated slurry. The encapsulation quality of the ground rubber was evaluated by SEM while the chemical influence on ASN was determined by EDS, FTIR, and XRD. Slipperiness change on the active surface of pavement stones proved that the addition of the ground rubber enhanced the walking safety of the product.

DOI
https://doi.org/10.18690/um.fkkt.1.2024.2

ISBN
978-961-286-829-1

Keywords:
waste rubber, alkali-activated metakaolin, encapsulation of organic in inorganic material, microwave irradiation, mechanical properties

University of Maribor Press

1 Introduction

Rubber represents a major challenge at the end of its life cycle due to its enormous quantities and recycling issues (Leong et al., 2023). Synthetic polymer (rubber) is used for tires, electrical cables, etc., and is made by the cross-linking process (vulcanization) (Coran, 2013). This crosslinking makes rubber more elastic (Flory, n.d.), which makes waste rubber interesting for recycling in construction materials as fillers (Nuzaimah et al., 2018). Its inclusion in various civil engineering products could provide many benefits, such as reducing stiffness and brittleness, improving the durability and longevity of the new composite material, dampening vibrations, and reducing road noise (Mutalib et al., 2021) while extending the life of the rubber and increasing the benefits to the users of the civil engineering product.

At the same time, the civil engineering and building industry consumes almost 70 $m_{\%}$ of the mass of Mount Everest in raw materials yearly and creates more than 30 $m_{\%}$ of global waste (Miller, n.d.). One of the solutions in this industry is to replace conventional materials, prepared from raw materials at high temperatures, like cement, with alkali-activated material (AAM) which is synthesized at temperatures lower than 100 °C and from materials that contain enough Si and Al in amorphous content, either as raw or waste material (Češnovar et al., 2019; Horvat et al., 2019a, 2019b, 2022a; Horvat and Ducman, 2019, 2020; Pavlin et al., 2021). Si and Al bind with O into tetrahedrons which are connected through O-bridges. This formation is called an aluminosilicate network (ASN) where the additional chemical bond of Al and O is compensated by the presence of elements from the 1st and the 2nd group of the periodic system (Škvára, 2007) which are introduced through alkalis.

Besides AAMs already having a lower impact on the environment when compared to conventional materials, the use of energy for their synthesis can be additionally lowered by replacing conventional (surface) heating with microwave irradiation (volumetric heating) (Horvat et al., 2023, 2022b). With volumetric heating, final mechanical strengths are reached in shorter times (Horvat et al., 2023), which decreases the time of the product from synthesis to the market leading to lower costs for the industry.

Combining both materials for driving/walking surfaces, i.e. coarsely ground waste rubber and AAM, would not just lower the impact on the environment but also result in the product with a less slippery surface, a quieter ride, and longer service life of the driving/walking surface, decrease the incidence of human falls and dampen the impact on the vehicle shock absorbers and human/animal joints, leading to higher quality life and better health.

In the paper, coarsely ground rubber was combined with alkali-activated metakaolin slurry as part of the active surface or spread throughout the volume, which has not yet been seen in the literature. The focus of the work was, besides testing improvement of samples being less slippery, on the quality of the encapsulation of the rubber in the ASN to avoid potential pollution through the back-spread of the ground rubber into the environment, not to cause additional "micro-plastic" issues.

2 Methods – evaluation of the material

Chemical evaluation of precursor metakaolin (MK) was performed by X-ray fluorescence (XRF; Thermo Scientific ARL Perform'X Sequential XRF) along with the determination of the amount of organic compound and carbonates through loss on ignition (LOI) for 2 hours at 550 °C and 950 °C, respectively.

Mineralogical analysis of MK, along with Rietveld refinement using external standard (corundum, Al_2O_3), was performed by X-ray powder diffraction (XRD; Empyrean PANalytical X-ray Diffractometer, Cu X-Ray source).

The precursor was dried, milled, and sieved below 125 μm for LOI, XRF, and XRD. Results were reported in our previous work (Horvat et al., 2023, 2022c) and also the optimal mixture of MK and used alkali (Na-silicate solution, Geosil, 344/7, Woelner, Ludwigshafen, Germany, 16.9% Na_2O, 27.5% SiO_2). The theoretically determined mass ratio (using software in MS Excel platform developed in project No. C3330-17-529032 "Raziskovalci-2.0-ZAG-529032" and upgraded in the ARRS project under Grant No. J2-3035) between MK and liquid alkali was 1:0.66, respectively. However, for the synthesis, MK was used as received (particle size distribution was evaluated by sieving through test sieves with mesh 5 mm, 4 mm, 2 mm, 1 mm, 0.4 mm, 0.125 mm, 0.09 mm, 0.063 mm).

On rubber waste from old electrical cables, received coarsely ground below 2 mm (particle size distribution was evaluated by sieving through test sieves with mesh 5 mm, 4 mm, 2 mm, 1 mm, 0.4 mm), thermogravimetric analysis and differential thermal analysis (TG/DTA; STA 409 PC Luxx, Netzsch, Germany) were performed in airflow from the room temperature to 1000 °C with a rate of 10 K/min to evaluate the temperature of ignition where the majority of the material would have already combusted. The rubber was ignited for 2 hours (LOI) at 550 °C (and at 950 °C) to determine the amount of ignition residual loss coming from the inside of the cables (conductive material, the metals, etc.), potential construction and demolition waste (Si, Al, and alkali (earth) metals), and inorganic content present in the rubber material. Rubber was evaluated by Fourier-transform infrared spectroscopy (FTIR; PerkinElmer Spectrum Two, ATR mode) where larger particles of different colour pigments were evaluated independently.

Besides FTIR performed on the rubber, it was performed also on MK powder, and on the ASN (along with the non-reacted MK) gently scratched with the spatula from the inside of the AAM (to exclude the rubber). For the XRD analysis of the ASN (and non-reacted MK), AAM was gently crushed in the mortar with the pastel and sieved below 0.4 mm to remove as much of the rubber as possible (XRD of the rubber sieved below 0.4 mm was performed, too).

On not polished and not coated MK powder, rubber (ignited for LOI determination and as received) and AAMs, scanning electron microscopy (SEM; Jeol JSM-IT500, low vacuum conditions) with energy-dispersive X-ray spectroscopy (EDXS; Oxford Instruments, Link Pentafet) was performed.

At 14 days of AAMs, geometrical densities along with mechanical strengths (bending and compressive) were measured. For the evaluation of mechanical strengths compressive and bending strength testing machine (ToniTechnik ToniNORM) was used.

3 Methods – synthesis of the material

Rubber was used as an active-surface partial cover (S) or volumetrically (V) spread in the alkali-activated metakaolin mixture (MK_b) in mass ratios presented in Table 1. For the one-surface partial cover, two different mass percentages of rubber were

used, i.e. 1.7 $m_{\%}$ (S_{min}) and 5.3 $m_{\%}$ (S_{max}) calculated on the mass of the metakaolin slurry while for volumetrically spread rubber, 9.0 $m_{\%}$ of rubber was used (also calculated on the mass of the slurry).

Table 1: Masses of the used ingredients.

Mixture	MK [g]	Alkali [g]	Rubber [g]
MK_b	50	33	/
S_{min}	50	33	0.7
S_{max}	50	33	2.2
V	50	33	7.5

For the volumetrical distribution of the rubber, rubber particles were homogenized with dry MK before being mixed with Na-alkali silicate solution until complete wetting and moulded into silicone-urethane rubber moulds of prisms measuring (2×2×8) cm^3.

For the one-surface rubber cover of the prism (measuring (2×2×8) cm^3), the bottom of the mould (measuring (2×8) cm^2) was partially (S_{min}) to almost fully (S_{max}) covered with coarsely ground rubber before fresh alkali-activated MK slurry was cast onto it. Casted slurries were manually pressed to help rubber particles penetrate them.

Three different curing procedures of all mixtures presented in Table 1 were evaluated: curing solely at room conditions (55% moisture, 22 °C) for 14 days, irradiating fresh slurry with microwaves (frequency 2.45 GHz, inverter microwave, i.e. microwaves are constantly on if chosen; Panasonic, NN-CD575M) for 1 min at 100 W (positively influencing the dissolution of reagents while dehydration is not severely affected (Horvat et al., 2023, 2022b)) or for 1 min at 1000 W (physical foaming of the slurry (Horvat et al., 2023, 2022b)), and additionally further curing all volumetrically heated specimens at room conditions for 14 days.

Each prism was irradiated separately in the 1st observed dosimetry maxima (approximately 6 cm away from the centre) without any cover on the moulds.

4 Methods – upscaling into pavement stones

Mixtures MK_b, S_{min}, and S_{max} (800 g of MK was used per pavement stone) were cast into moulds with a bottom surface measuring (20×20) cm². Rubber was uniformly spread either on the bottom of the mould or all over the top of the slurry. Rubber in mixture S_{max} was uniformly spread over the mesh (cut into the PVC foil placed directly onto the slurry) of 2 cm wide stripes that were 2 cm apart.

On the top of all casted mixtures with/without the rubber, PVC foil was placed onto which stone measuring (20×20) cm² with a smooth surface and weighting 3 kg was laid (the whole procedure up to placing the smooth stone is shown in the Supplement in Figure S1). Besides the stone offering uniformly distributed pressure onto the slurry, additional force, 2.5 kN, was introduced with a compressive and bending strength testing machine pressing onto the stone (HPM 25/5, Zavod za raziskave materiala in konstrukcij Ljubljana). Pressure onto the layer of the rubber is presented in Table 2 and depends on the placement of the rubber and the masses/forces above it (forces presented onto the rubber sum up).

Table 2: Pressure onto the rubber.

Source of the pressure onto the surface (20×20) cm²	Slurry 1.3 kg [kPa]	Stone 3 kg [kPa]	Additional force 2.5 kN [kPa]
Rubber on the bottom	0.32	0.76	62.50
Rubber on the top	/	0.76	62.50

Pavement stones were cured solely at room conditions and de-moulded 1 hour, 2 hours, 24 hours, and 48 hours after casting alkali-activated slurries. The stone on top of the PVC foil was removed just before de-moulding.

Change in the slipperiness of the active surface of the pavement stone was tested according to the SIST-TS CEN/TS 16165 Annex C to test the influence of the addition of the ground rubber regarding the accident safety of the product.

The contact surface area at the test measures 95.76 cm² while for striped pavement stone, the contact area splits into the contact area with AAM and the contact area with rubber. If the pendulum slides over striped pavement stone perpendicular to the stripes, the contact area with rubber is 45.60 cm² (50.16 cm² with AAM) but if

the pendulum slides over striped pavement stone along the stripes, the contact area with rubber is 50.40 cm² (45.36 cm² with AAM).

5 Results – materials used

Particle size distributions of MK and coarsely ground rubber along with their photographs are presented in Figure 1. While MK has more than 90 m% of particles below 0.09 mm, coarsely ground rubber has 80 m% of particles bigger than 0.4 mm.

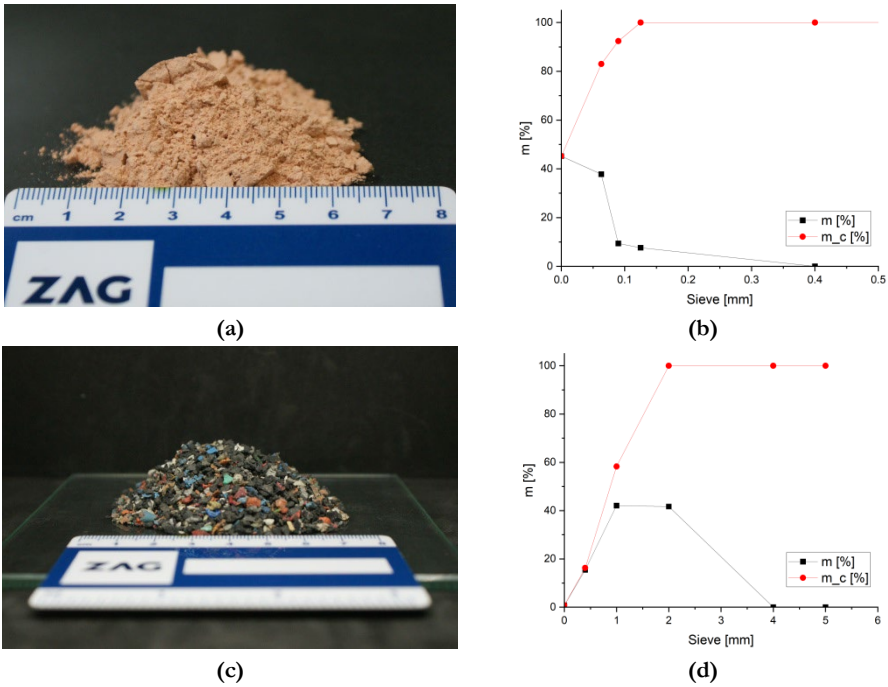

Figure 1: (a) MK and (c) coarsely ground rubber, with their particle size distribution (b) and (c), respectively.
Source: own.

Thermal analysis performed on the rubber and used to determine the temperature where the majority of the organic material is removed is shown in Figure 2. The majority combusts up to 550 °C where rubber leftover becomes black. However, the mass loss continues further on, leaving the material light grey (white) at 950 °C.

SEM micrographs of MK and rubber are presented in Figure 3 and their EDXS analysis is in Table 3 (areas of the acquisition on the rubber are in the Supplement in Figure S2). From SEM micrographs of MK, it is clear that the precursor used in the synthesis is a fine powder of uniform chemistry (the greyscale of the particles is narrow). However, rubber is the complete opposite, i.e. besides the majority of the rubber particles being tremendous for observation under SEM even at lower magnifications (Figure 3 (b_i/b_{ii})). Its smaller fraction (Figure 3 (c)) shows severe non-uniformity in size, shape, and chemistry, which is presented in Table 3 according to the greyscale level of the waste rubber/"rubber" particles and their shape. After ignition at 550 °C, rubber showed severe deterioration (Figure 3 (d_i)) with few less damaged areas (Figure 3 (d_{ii})). Nonetheless, it was easy to crush all larger rubber particles into powder with just a gentle pressing with a spatula (Figure 3 (e)). Ignition of rubber at 950 °C left no undamaged parts of the rubber (Figure 3 (f)), and the remaining rubber was easily crushed with a spatula to powder (Figure 3 (g)).

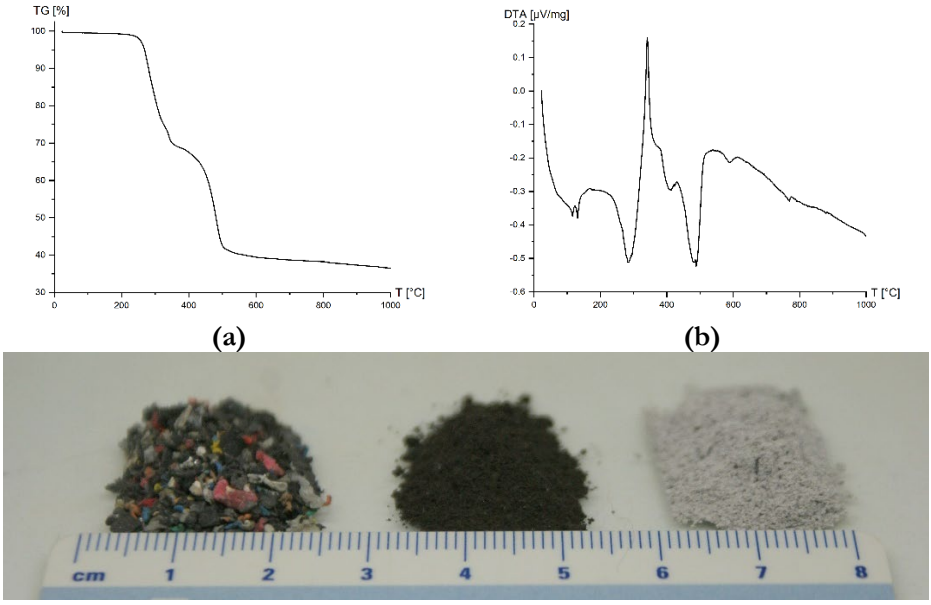

Figure 2: (a) TG and (b) DTA of coarsely ground rubber. (c, from left to right) Rubber before ignition, rubber after ignition at 550 °C (crushed with a spatula), and after 950 °C (crushed with a spatula).

Source: own.

While MK consists mostly of Si and Al (and Fe, hence the orange-red colour of the MK powder), coarsely ground rubber from electric cables is much more than just organic polymer, i.e., it contains also conductive elements present in the metallic wires of electric cables and also elements that are present in construction materials surrounding electric cables in the walls. However, non-rubber materials (plates, fibres), even metallic, are hard to find under SEM (Figure 3 (e-1)), which means that their $m_{\%}$ is low, but are all present and not affected by thermal treatment.

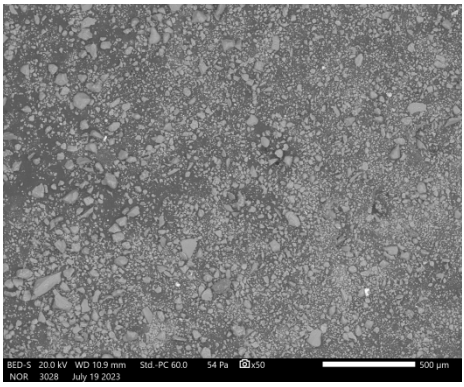

(a-1)

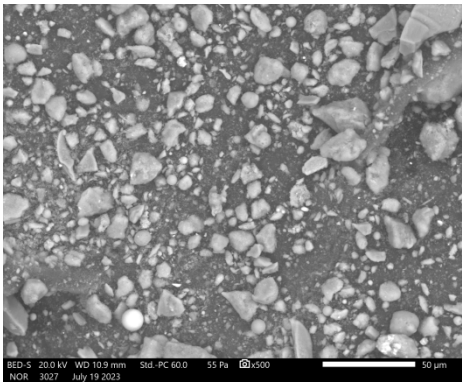

(a-2)

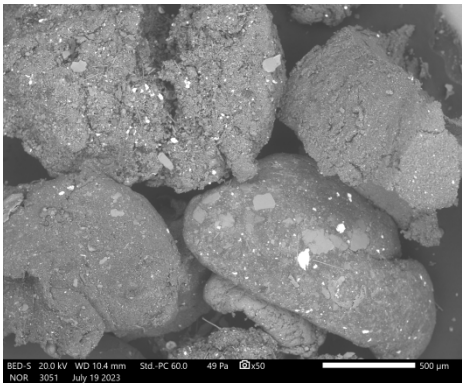

(b_i-1)

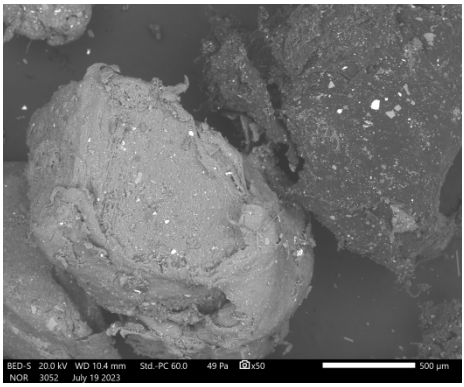

(b_{ii}-1)

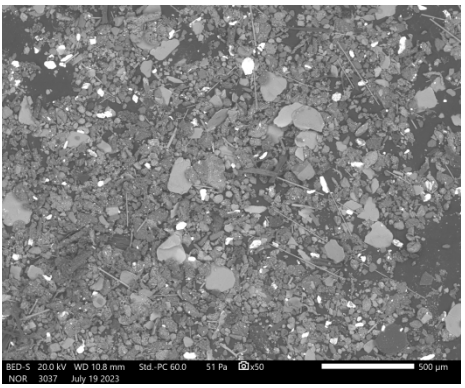

(c-1)

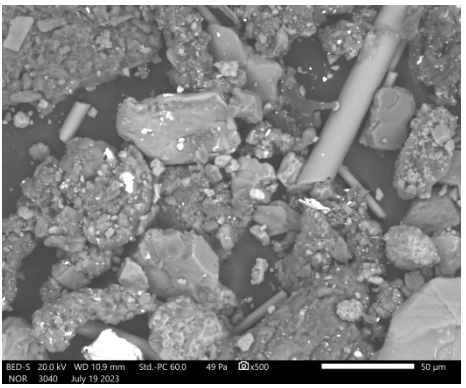

(c-2)

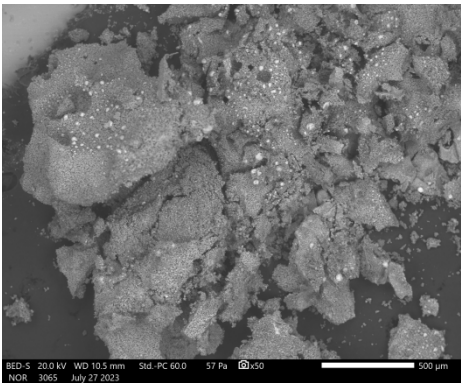

(d_i-1)

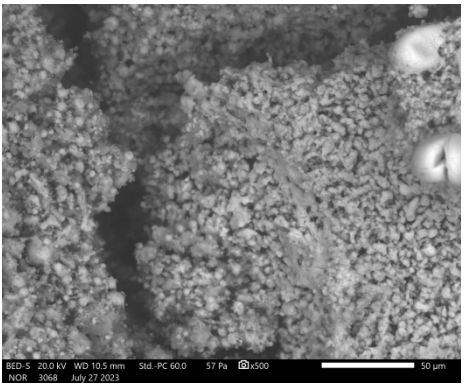

(d_i-2)

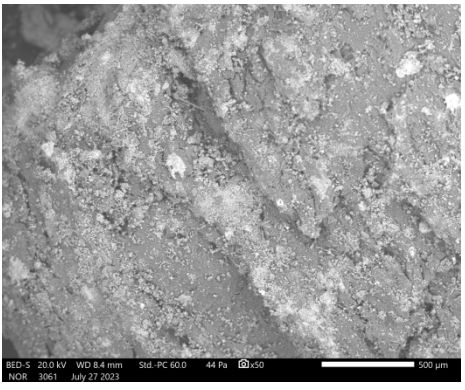

(d_{ii}-1)

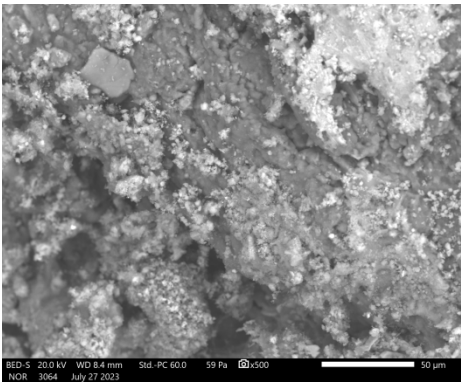

(d_{ii}-2)

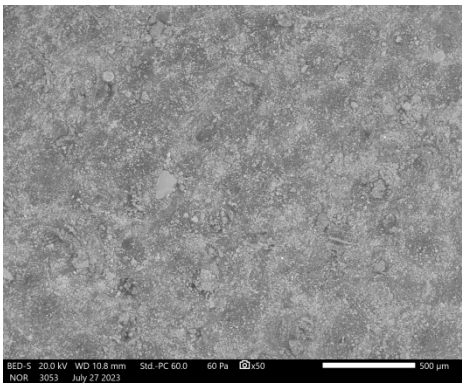

(e_i-1)

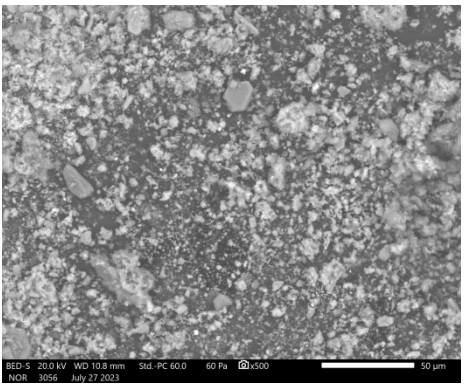

(e_i-2)

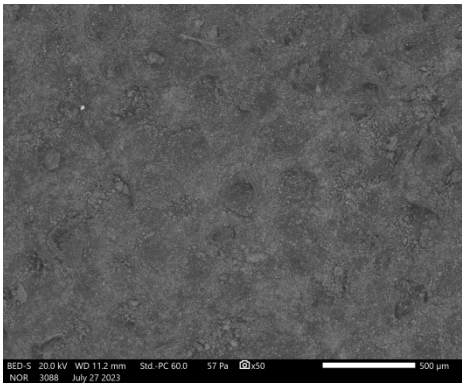

(e_{ii}-1)

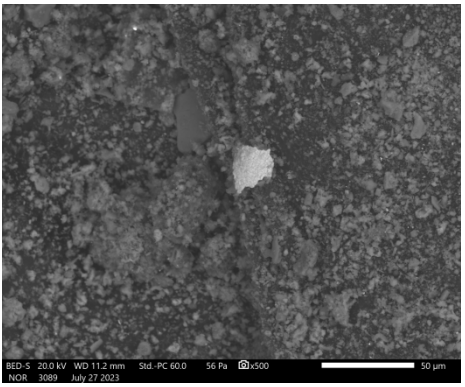

(e_{ii}-2)

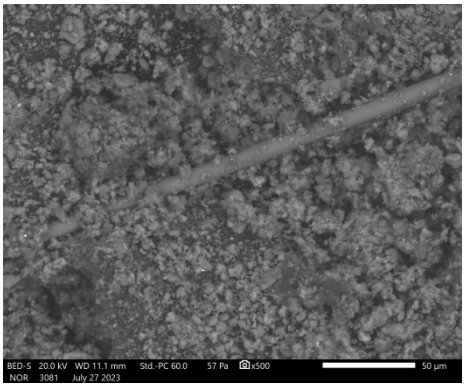

(e_{iii}-2)

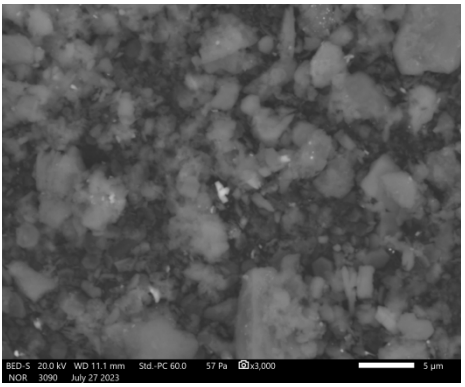

(e-3)

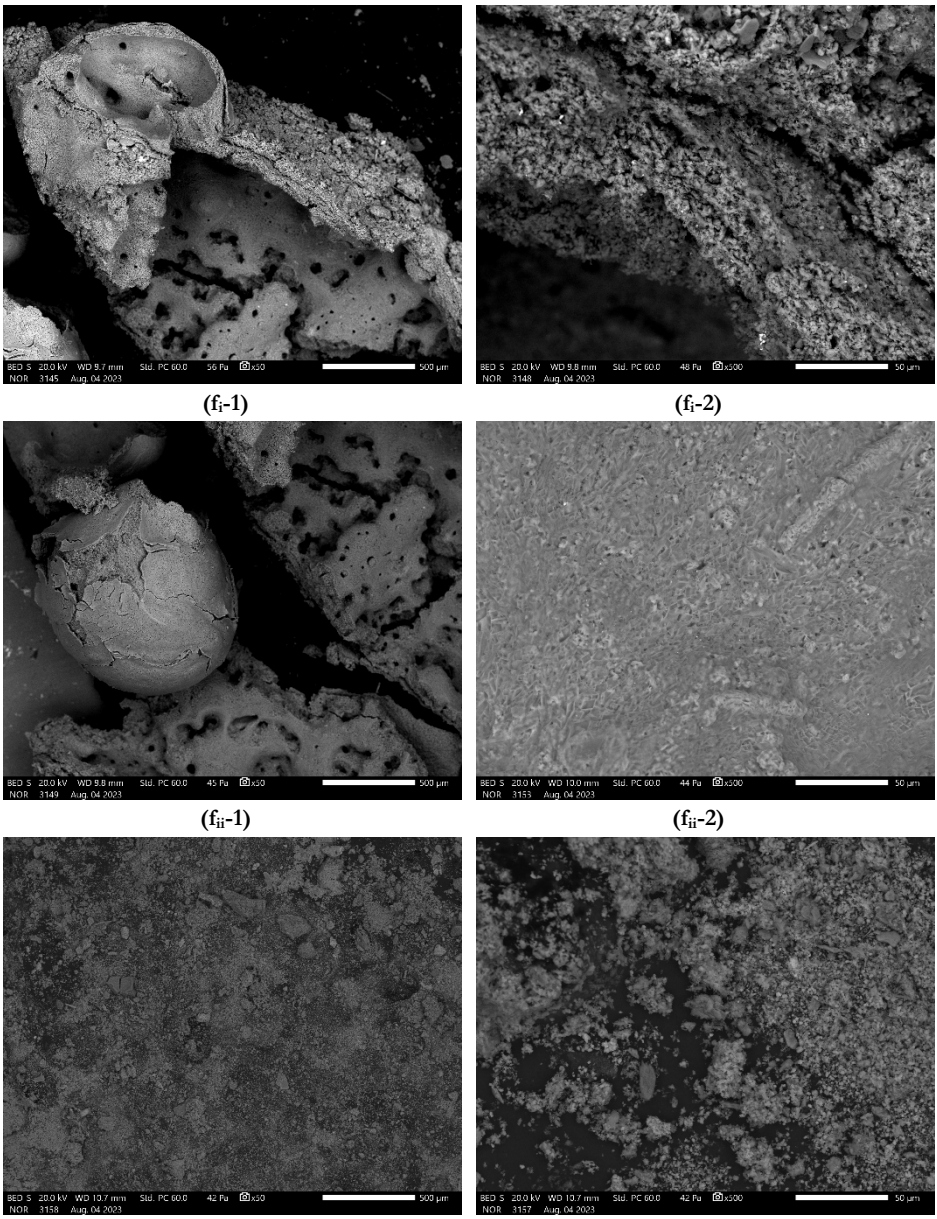

(f_i-1) **(f_i-2)**

(f_{ii}-1) **(f_{ii}-2)**

(g-1) **(g-2)**

Figure 3: SEM micrographs of (1) 50-times, (2) 500-times and (3) 3000-ground magnified (a) MK, (b) coarsely ground rubber, (c) finer fraction of coarsely ground rubber, (d) rubber ignited at 550 °C which was (e) gently crushed with a spatula, (f) rubber ignited at 950 °C which was (g) gently crushed with a spatula. (i, ii, iii) indicate additional micrographs on the same sample with the same magnification.

Source: own.

Thermal treatment of rubber at 550 °C removed 41.45 m% of organic material (LOI at 550 °C for MK is just 1.29 m%) while increasing the m% of Cl (Table 3). However, Si and Al present in ignited material, not encapsulated anymore by organic material that does not react with alkali (Afshinnia and Poursaee, 2015), could now be at least partially reactive in alkali and contribute to ASN formation. Thermal treatment of coarsely ground rubber at 950 °C decreased mass by an additional 25.21 m% (0.77 m% for MK), i.e., the whole mass loss at 950 °C was 66.31 m% (2.06 m% for MK). Higher ignition temperature increased the amount of Cl, i.e., Cl could not be removed with thermal treatment up to 950 °C (it must be chemically bound in the system).

FTIR measurements of MK, Geosil, and distilled water, all crucial in alkali-activated synthesis, along with the larger rubber particles of different colours and rubber ignited at 550 °C and gently crushed with a spatula, are presented in Figure 4. From all materials present in the final product, alkali and MK contributed to the formation of ASN, according to XRF and XRD analysis of MK (Horvat et al., 2023, 2022b), to EDXS evaluation, and according to FTIR results, where not just for MK but also for the alkali (Geosil), peak (pink circle in Figure 4) indicating the presence of Si-O-Al and/or Si-O-Si bonds is present. FTIR of rubber ignited at 550 °C shows no resemblance to rubber before ignition, leading to the conclusion that bonds in the rubber degraded under temperature (as can be seen in SEM micrographs in Figure 3). As from EDXS results (Table 3), also from FTIR results of ignited waste coarsely ground rubber, ignited rubber might have the potential to be used in alkali-activation synthesis as a precursor or at least as a reactive filler because of the wide peak marked in a pink square in Figure 4. If the peak is narrow and sharp, the peak would indicate the presence of crystalline material. Because it is wide, however, it has the potential to contain amorphous content consisting of a material having Si-O-Al and Si-O-Si bonds which are crucial for ASN formation.

Worth mentioning is also that rubber ignited at 550 °C and 950 °C becomes severely hydroscopic, i.e., droplets cover the surface of the powder pressed in the XRD sample holder after being left at room conditions for a few days. The hydrophilic nature of the ignited rubber can be seen also in Figure 4 where this effect was additionally followed by FTIR on pulverized rubber ignited at 950 °C (Figure 4 (b)) while the material was exposed to room conditions during the FTIR measurement.

Table 3: Average EDXS of MK and rubber in mass percentage ($m_{\%}$) and atomic percentage ($a_{\%}$) without C, O, and elements below 0.1 $m_{\%}$.

Elements [$m_{\%}$]	Shade	Si	Al	Na	K	Ca	Mg	Ti	Fe	Cu	Zn	Sn	Ba	Pb	S	Cl	F
MK	Uniform	14.8	13.3		0.1	0.2		0.5	4.4								
Rubber fine	White	0.4	0.9			0.5	0.9	0.1	3.6	21.5	3.4	12.8	0.9		0.2	0.2	
	Light grey plates	11.0	4.8	0.5	3.8	1.1	8.6	0.2	1.0	0.3			0.1			0.2	2.9
	Middle grey random	1.7	2.8		0.2	6.0	8.2		0.3	1.3	0.5	0.1				1.7	
	Dark grey plates	1.3	0.7		0.1	1.9	1.9		0.2	0.5	1.0	0.6	0.1		0.2	0.4	
	Middle grey fibres	10.6	4.0	0.2	0.2	8.8	1.8	0.1	0.2	0.4						0.2	0.2
Rubber coarse	Light grey	0.4	1.1			3.8	1.1			0.2	0.1					7.3	
	Middle grey	2.6	3.8		0.4	3.7	4.0		0.3	0.3	0.5			0.1		0.5	0.1
	Dark grey		0.6			0.3	0.1										
Rubber fine 550 °C	White	0.3	0.7			0.3			0.3	19.1	0.5				3.7	0.4	
	Light grey	3.3	5.4	0.1	0.4	3.5	10.5		0.3	0.1	0.6		0.5		0.1	5.0	0.1
	Middle grey	2.4	3.7	0.1		3.9	2.1		0.1	0.2	0.5				0.1	5.5	
	Dark grey plates	0.7	21.2	0.2		1.0	1.0			0.2	0.6					1.1	
Rubber coarse 550 °C	Light grey	1.3	2.9			7.2	0.8		0.2	0.2	1.2			0.5		10.6	
	Grey	2.3	4.1		0.1	3.8	1.3		0.3	0.3	1.6				0.3	3.1	
Rubber coarse 950 °C	Light grey	1.0	1.1		0.2	14.7	9.6		0.2	0.3	0.5				0.2	21.6	
	Grey	7.4	7.4	0.2	0.8	17.8	0.9		0.4	0.6	3.0				0.2	5.8	
Elements [$a_{\%}$]	Shade	Si	Al	Na	K	Ca	Mg	Ti	Fe	Cu	Zn	Sn	Ba	Pb	S	Cl	F
MK	Uniform	9.5	8.9		0.1	0.1		0.2	1.6								
Rubber fine	White	0.4	0.8			0.3	0.9	0.05	1.6	7.8	1.2	2.9	0.1		0.1	0.2	
	Light grey plates	7.0	3.2	0.4	1.8	0.5	6.4	0.06	0.3	0.08			0.02			0.1	2.8
	Middle grey random	1.1	1.7		0.1	2.7	5.7		0.1	0.3	0.1	0.02				0.8	
	Dark grey leafs	0.7	0.4		0.04	0.7	1.3		0.04	0.1	0.2	0.08	0.01		0.09	0.2	
	Middle grey fibres	6.7	2.6	0.2	0.1	3.9	1.3	0.04	0.08	0.1						0.1	0.2
Rubber coarse	Light grey	0.2	0.7			1.6	0.7			0.06	0.04					3.3	
	Middle grey	1.5	2.2		0.2	1.5	2.7		0.1	0.07	0.1			0.01		0.3	0.1
	Dark grey		0.3			0.1	0.08										
Rubber fine 550 °C	White	0.2	0.5			0.2			0.1	5.5	0.1				2.1	0.2	
	Light grey	2.0	3.5	0.06	0.2	1.6	7.5		0.1	0.03	0.2		0.07		0.07	2.5	0.08
	Middle grey	1.4	2.2	0.06		1.6	1.4		0.03	0.05	0.1				0.04	2.5	
	Dark grey plates	0.4	13.5	0.2		0.4	0.7			0.05	0.2					0.5	
Rubber coarse 550 °C	Light grey	0.8	1.8			3.1	0.5		0.07	0.07	0.3			0.04		5.18	
	Grey	1.3	2.5		0.05	1.6	0.9		0.08	0.08	0.4				0.2	1.5	
Rubber coarse 950 °C	Light grey	0.7	0.8		0.1	7.6	8.2		0.07	0.1	0.2				0.1	12.6	
	Grey	5.3	5.6	0.1	0.4	9.0	0.8		0.1	0.2	0.9				0.1	3.3	

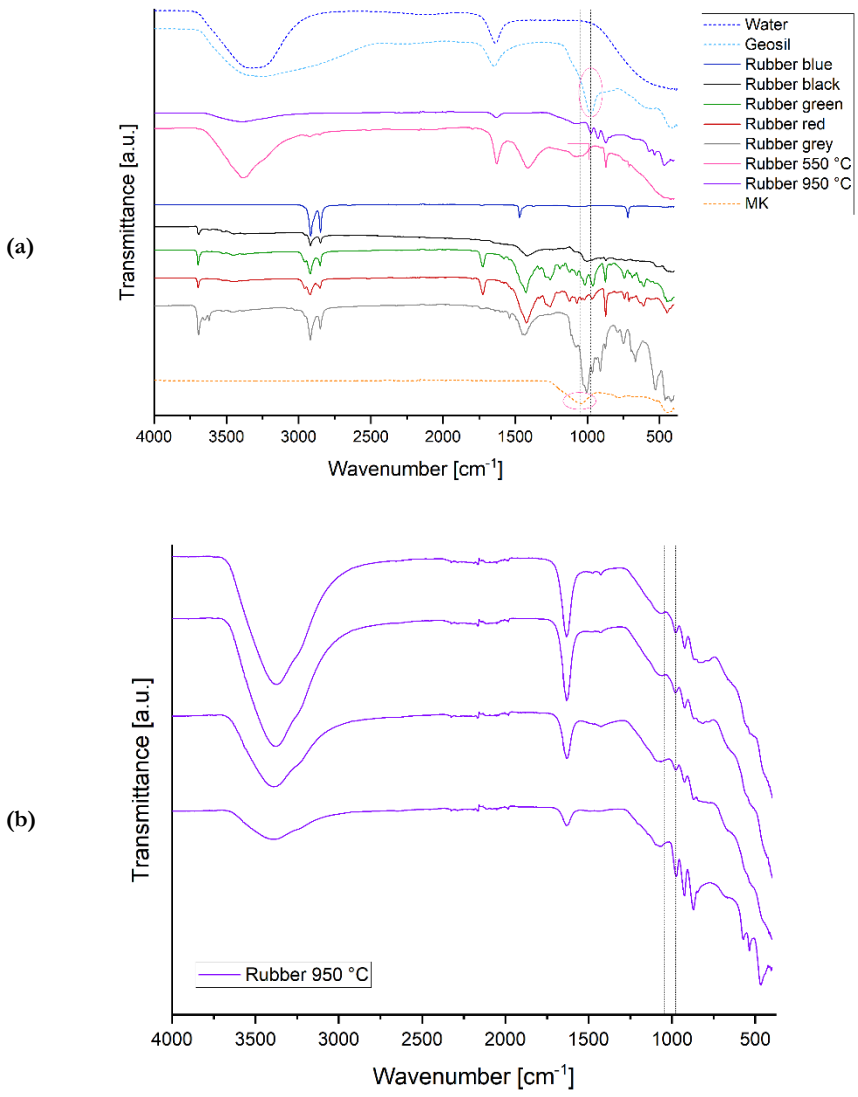

Figure 4: FTIR of (a) MK, alkali (Geosil), distilled water, larger particles of rubber of different colours, and rubber ignited at 550 °C and 950 °C. Circles denote peaks relevant to ASN formation while square denotes a potentially relevant peak for ASN formation. (b) FTIR of rubber ignited at 950 °C measured with shorter-longer exposure to room conditions (bottom to upper curve respectively).

Source: own.

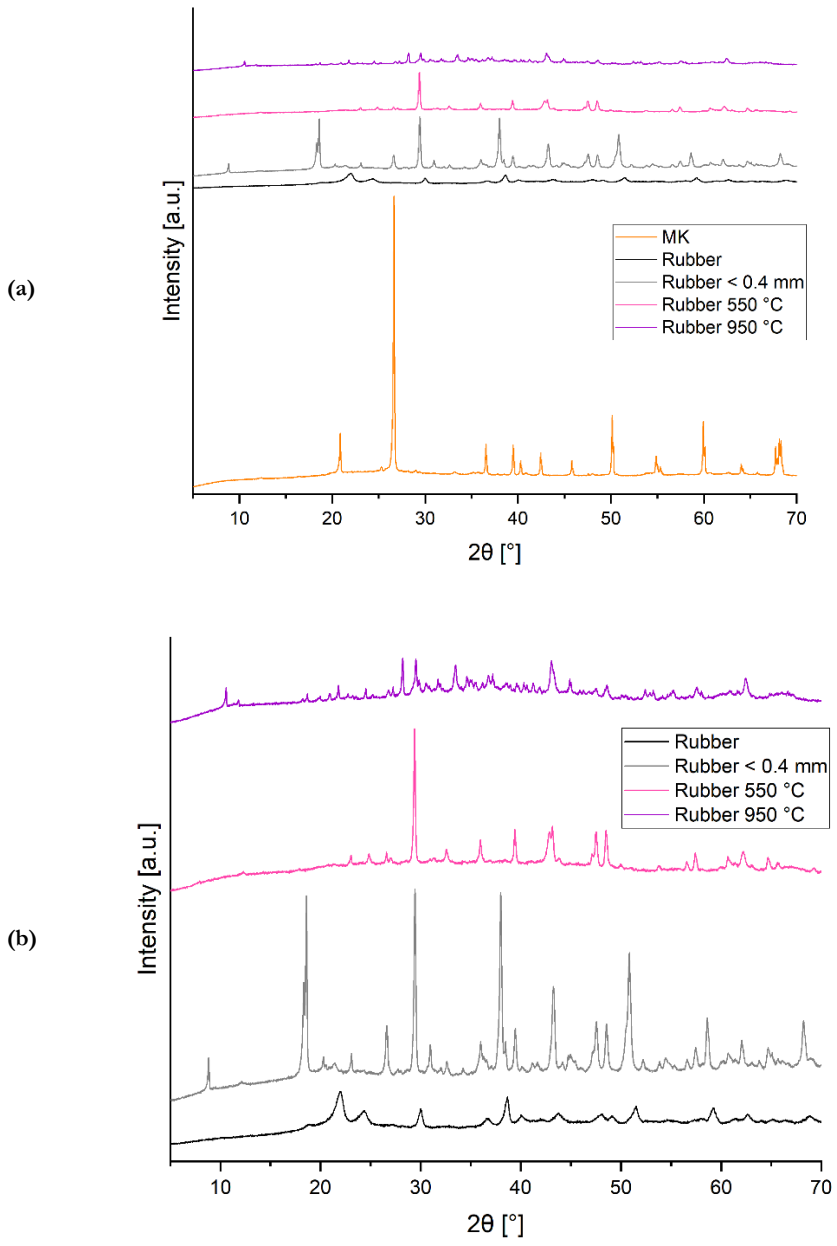

Figure 5: XRD of (a) MK, rubber as received, rubber sieved below 0.4 mm and rubber ignited at 550 °C and 950 °C crushed with a spatula, and XRD of (b) rubber solely.

Source: own.

The longer the exposure, the more prominent the water peaks (between 3000 cm^{-1} and 3500 cm^{-1}, and 1550 cm^{-1} and 1700 cm^{-1}), i.e., the bottommost curve was performed first (this curve is also shown in Figure 4 (a) while FTIR of rubber ignited at 550 °C was measured after longer exposure to room conditions).

XRD of MK and rubber (as received, fraction smaller from 0.4 mm, ignited at 500 °C and 950 °C) is shown in Figure 5. While waste coarsely ground rubber was not optimally prepared for XRD measurement (milled and sieved below at least 125 μm), it still showed crystal structure. However, its fraction, smaller from 0.4 mm, had more and more prominent peaks. While some peaks are in common with rubber ignited at 550 °C and 950 °C, the difference between all rubber patterns is noticeable.

6 Results – laboratory scale AAM

The curing procedure (treatment solely at room conditions, or also with microwaves with lower/higher power)) did not affect the adhesion of the rubber to alkali-activated metakaolin slurry but the amount of the rubber did (Figure 6). While the amount of rubber used for S_{max} was too big (excess rubber is easily removed before using the product), the amount of rubber in S_{min} could still be increased.

(a) **(b)**

Figure 6: 14-day-old samples with the surface distribution of the rubber before and after mechanical tests. Left to right: S_{min}/S_{max} cured solely at room conditions, S_{min}/S_{max} cured with microwaves for 1 min at 100 W, S_{min}/S_{max} cured with microwaves for 1 min at 1000 W.
Source: own.

In the case of the use of a bigger amount of rubber particles (S_{max}), slurry did not come in contact with all the rubber particles while in the case of a smaller amount of rubber particles (S_{min}), rubber particles got at least partially encapsulated into the

alkali-activated metakaolin slurry leaving no option for the rubber particles to be redistributed back to the environment (if the alkali-activated material does not get affected by aging and weather). However, this means not only that the amount of uniformly distributed rubber particles is important but also the force with which slurry (with certain rheological parameters) is pressed onto the rubber particles.

While curing with microwaves at 1000 W, slurry pulled the rubber even deeper inside into the prism, but at the lower energy of microwaves, the depth of the rubber particles was influenced solely by the pressure while moulding. This means that adhesion forces between the alkali-activated metakaolin slurry and rubber particles were strong enough for the rubber to move with the slurry while it was physically foamed (microwave irradiation at 1000 W) (Horvat et al., 2023, 2022b) and in this way, rubber did not negatively influence the newly formed bonds in the alkali-activated material.

As in the case of the surface distribution of the rubber particles, it is also in the case of their volumetric distribution (Figure 7), i.e., the adhesion of the rubber particles with metakaolin slurry, regardless of the curing, was satisfactory. It is almost impossible for the rubber particles to be distributed back into the environment, even more, cutting alkali-activated metakaolin foam on its sides (slurry cured with microwaves at 1000 W, 3rd prism from the left in Figure 7) did not pull rubber particles out from the alkali-activated foam but cut them just as the alkali-activated foam's skeleton was cut (most right prism in Figure 7 (a)).

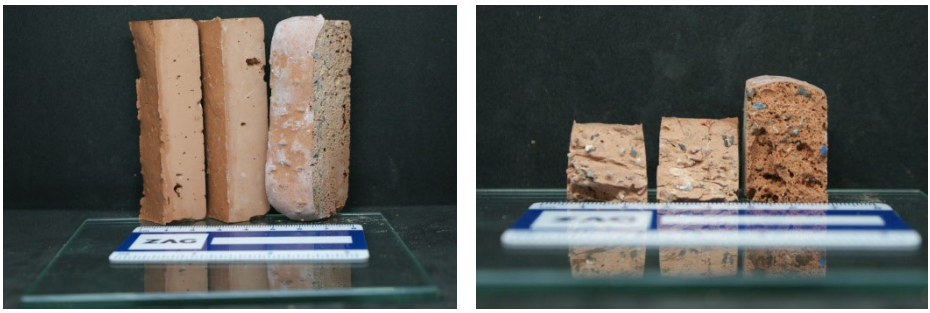

(a) **(b)**

Figure 7: 14-day-old samples with the volumetric distribution of the rubber before and after mechanical tests. Left to right: V cured solely at room conditions, V cured with microwaves for 1 min at 100 W, and V cured with microwaves for 1 min at 1000 W.

Source: own.

Mechanical strengths (compressive and bending) and the geometrical densities of 14-day-old samples are shown in Figure 8. Densities are affected by the addition of the rubber particles but this effect is lesser when compared to non-foamed (curing at room conditions and with microwaves at 100 W) and foamed (microwave irradiation at 1000 W) alkali-activated metakaolin. Compressive strength is higher if samples were cured with microwaves at 100 W due to enhancement in the dissolution of ingredients, and the smallest if samples were cured with microwaves at 1000 W due to the foaming effect (Horvat et al., 2023, 2022b). A logical decrease in compressive strength occurs when rubber is volumetrically spread while the not-expected higher compressive strength happens in the surface addition of a higher amount of rubber particles.

SEM micrographs of AAMs with a focus on the encapsulation of the rubber in the AAM with volumetrically spread rubber are shown in Figure 9. In samples cured at room conditions and at 100 W for 1 min, all rubber particles were at least partially covered with random-shaped, sharp-edged particles of a similar grey shade as the ASN and also as the non-reacted parts of MK. Those particles are found also in the holes where rubber particles were located (Figure 9 (b-1)).

The sample that was treated at 1000 W for 1 min (Figure 9 (c)), which was enough for the sample to foam and completely harden, was enough also for the encapsulation of the rubber by completely trapping it in the AAM but had just a few rubber particles that had a new layer on their surface, i.e., under SEM, they were very hard to find (Figure 9 (c_i)). On the other hand, for samples treated solely at room conditions or at 100 W for 1 min, rubber without a significant amount of less organic particles on its surface was hard or impossible to find.

Semi-quantitative chemical analysis, EDXS, of the ASN and rubber is presented in Table 4 (areas of the acquisition of the signal are shown in the Supplement Figure S3). As elemental composition in the ASN can be compared among samples cured with different procedures, so can be elemental composition acquired on the rubber with the greyish surface, which is just a bit darker grey than ASN itself. However, particles present on the surface of the rubber are chemically comparable to ASN and not to the rubber with the greyish layer.

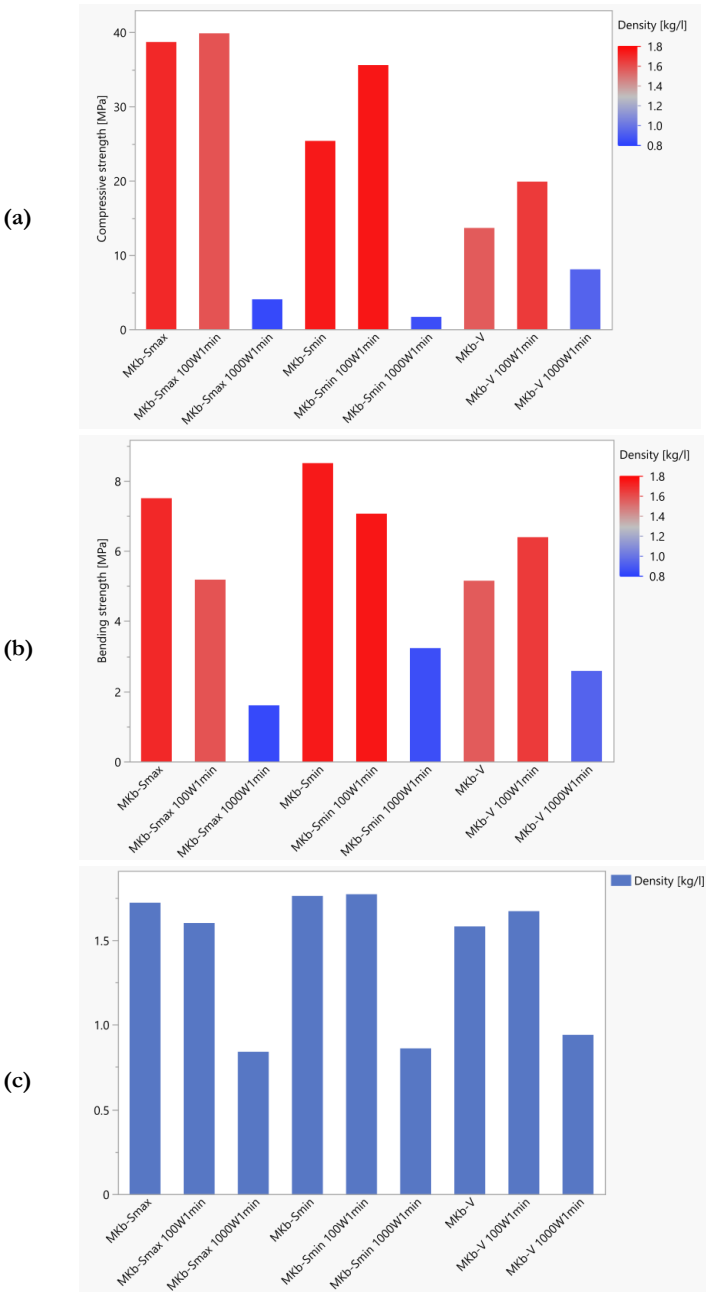

Figure 8: Mechanical strengths and geometrical density of 14-day-old samples.

Source: own.

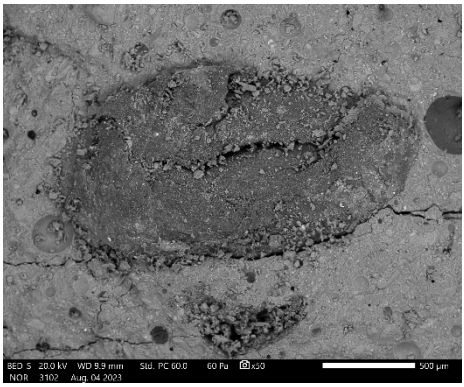

(a-1)

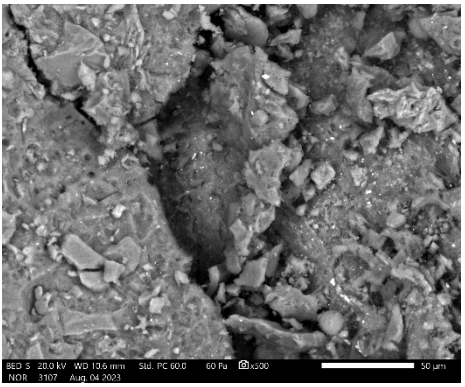

(a-2)

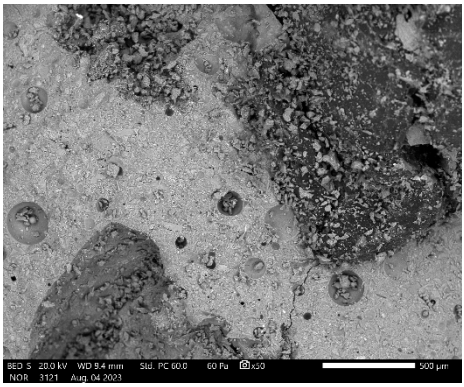

(b-1)

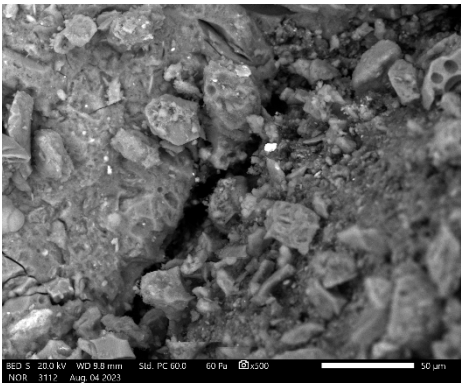

(b-2)

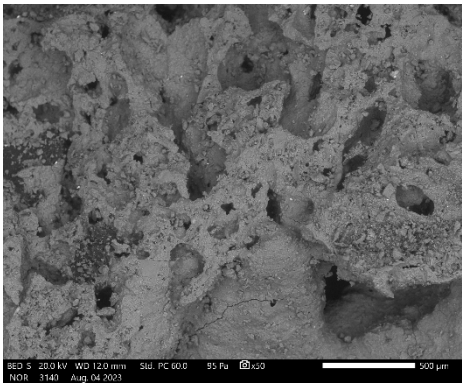

(c-1)

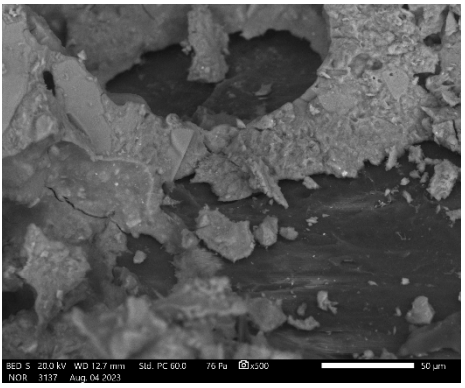

(c-2)

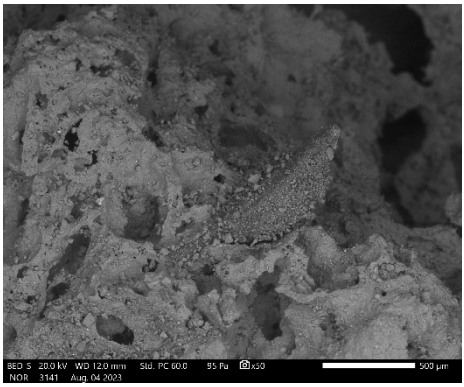

(c_i-1)

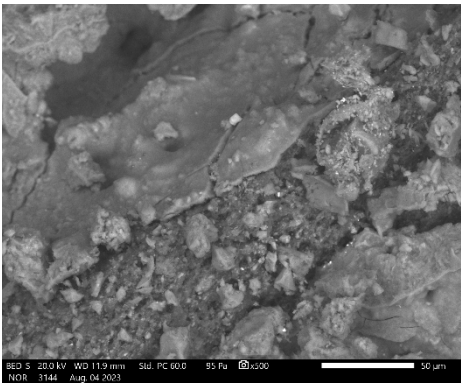

(c_i-2)

Figure 9: SEM micrographs of AAMs with volumetrically spread rubber (V) cured at (a) room conditions, (b) at 100 W for 1 min, and (c, c_i) 1000 W for 1 min where micrographs are (1) 50-times and (2) 500-times magnified.

Source: own.

Table 4: Average EDXS of AAM in mass percentage ($m_{\%}$) and atomic percentage ($a_{\%}$) without C, O, and elements below 0.1 $m_{\%}$.

Elements [$m_{\%}$]	Si	Al	Na	K	Ca	Mg	Ti	Fe	Cu	Zn	W	Cl
ASN V T_0	20.3	10.6	7.0	0.1	0.4		0.5	1.0				0.1
Rubber layer V T_0	2.6	7.1	1.0	0.1	2.0	1.3	0.1	0.3	0.3	0.1		0.6
ASN V 100W	20.0	7.5	5.4	0.1	0.3		0.3	2.2			0.3	
Rubber layer V 100W	4.2	3.0	1.3	0.1	0.5	0.2		0.3		0.3		
Particle on rubber V 100W	16.1	9.1	6.1	0.1	0.8		0.4	1.0			0.1	
ASN V 1000W	16.3	7.4	8.8		0.5		0.4	1.0				
Rubber layer V 1000W	7.8	4.9	5.5	0.2	1.9		0.3	0.5		0.3		0.1
Rubber dark V 1000W	0.3	0.1	0.3									
Elements [$a_{\%}$]	Si	Al	Na	K	Ca	Mg	Ti	Fe	Cu	Zn	W	Cl
ASN V T_0	13.5	7.3	5.7	0.05	0.2		0.2	0.3				0.06
Rubber layer V T_0	1.5	4.2	0.7	0.05	0.8	0.9	0.04	0.09	0.08	0.03		0.3
ASN V 100W	13.1	5.1	4.3	0.05	0.1		0.1	0.7			0.03	
Rubber layer V 100W	2.4	1.7	0.9	0.05	0.2	0.2		0.08		0.07		
Particle on rubber V 100W	10.3	6.1	4.7	0.06	0.3		0.1	0.3				
ASN V 1000W	10.4	4.9	6.8		0.2		0.1	0.3				
Rubber layer V 1000W	4.7	3.1	4.1	0.09	0.8		0.1	0.1		0.07		0.06
Rubber dark V 1000W	0.2	0.08	0.2									

FTIR of all AAMs (while trying to exclude the rubber at the sample preparation), presented in Figure 10, shows similar behaviour for AAMs cured in the same manner no matter the addition of the rubber. The higher the energy input into the curing, the lower the presence of the water (peak between approximately 3000 cm^{-1} and 3600 cm^{-1}, and peak with minima around 1640 cm^{-1}) and the shift of the minima of the "ASN" more towards the MK (to the left), i.e., away from the "ASN" peak of the alkali.

For XRD measurement AAMs were crushed in mortar with pastel and sieved below 0.4 mm to remove at least larger rubber particles. All patterns are similar (Figure 11), showing impact from MK, which means that at least the majority of the rubber particles were successfully removed, i.e., they were removed beyond detection. As reported before, curing at room temperature solely or also with microwaves does not affect alkali activation on a crystalline level (Horvat et al., 2022c). The same does not addition of rubber.

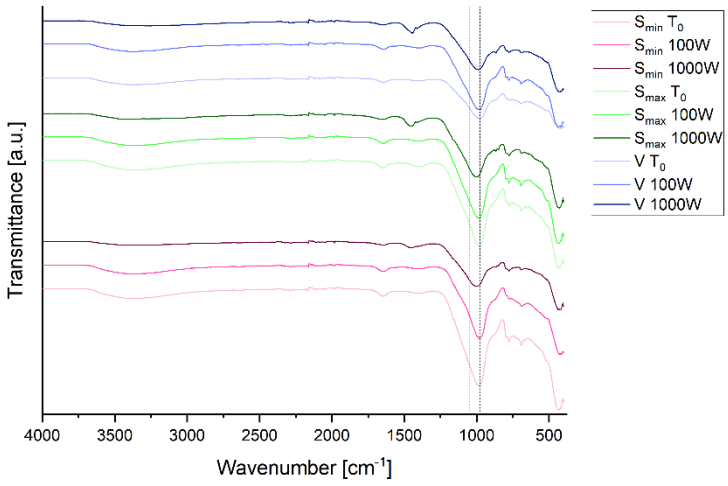

Figure 10: FTIR of AAMs (S_{min}, S_{max}, V) cured at room conditions (T_0), and for 1 min at 100 W or 1000 W. Vertical dotted lines represent "ASN" peak minima for MK (left) and alkali (right).

Source: own.

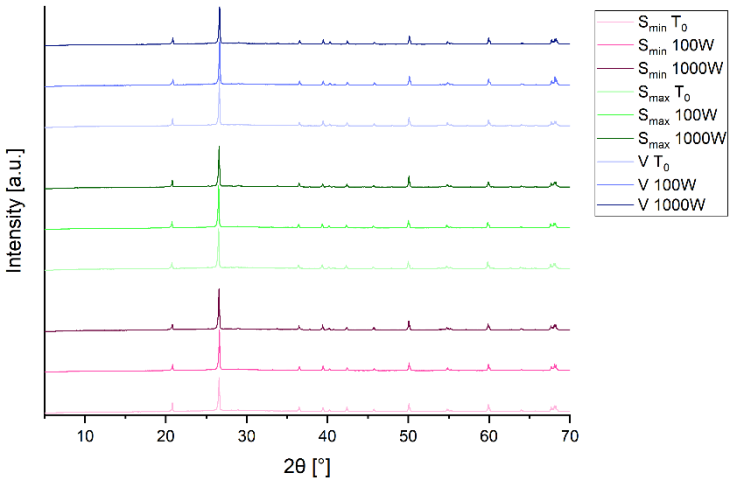

Figure 11: XRD of AAMs (S_{min}, S_{max}, V) cured at room conditions (T_0), and for 1 min at 100 W or 1000 W.

Source: own.

7 Results – pilot products

Upscaling of material presents additional challenges that can not be spotted on a laboratory scale, i.e., the path to perfect pavement stones is presented in Figure 12, and the Supplement in Figure S1. If de-moulding was too early (Figure 12 (a)), the bottom surface of the AAM was rough, with bubbles and the pavement stone was curved. If samples were de-moulded at least 2 hours after moulding (Figure 12 (c)), "slurry" was already hardened enough and could not be inflicted by the gentle de-moulding. However, samples that were de-moulded 24 hours after casting the slurry into the moulds were completely hardened and could not be inflicted by de-moulding at all.

Besides pavement stones having no curvature, if de-moulding was done later, the constantly present load on top of the slurry resulted in pavement stone having a smooth shiny surface where there were no (or hardly any) bubbles seen (Figure 12 (b)).

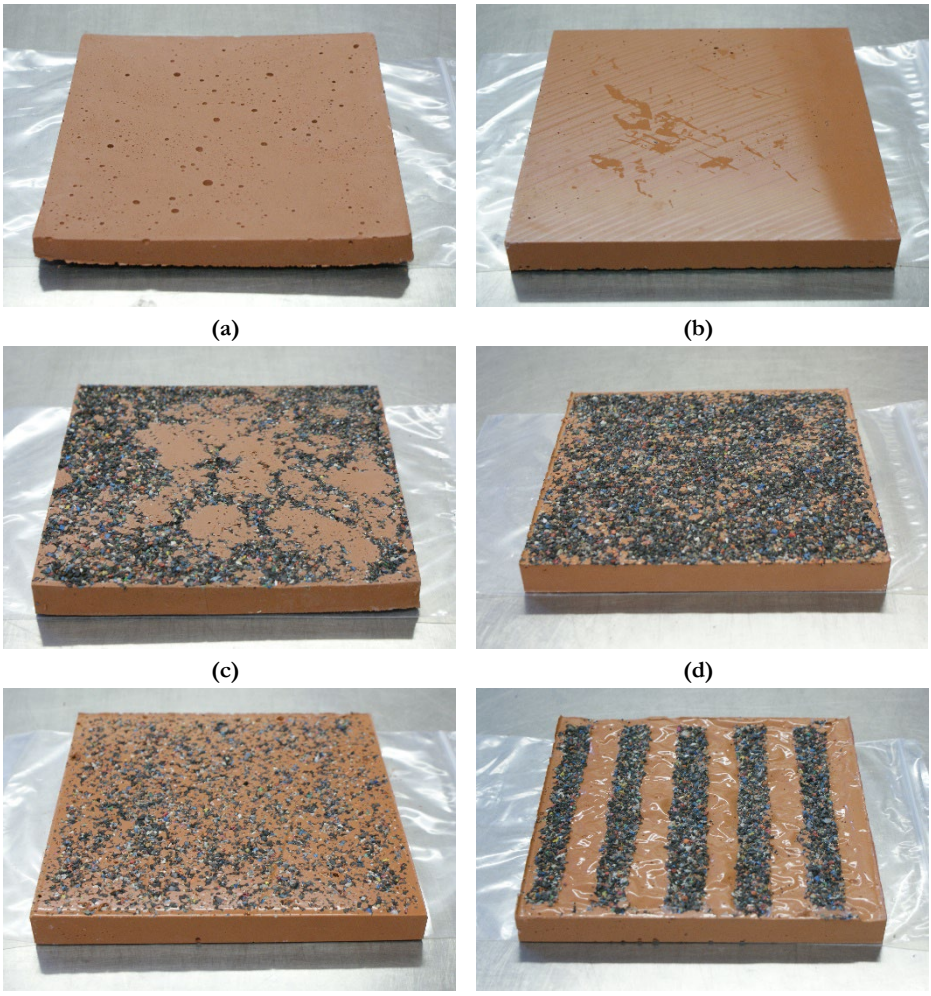

Figure 12: (a) MK_b de-moulded after 1 hour, and (b) after 24 hours, both pressed with "stone". (c) S_{max} with rubber particles on the bottom and pressed with the highest used force, de-moulded after 2 hours. De-moulded after 24 hours (d) S_{max} with rubber particles on the top and pressed with "stone", (e) S_{min} with rubber particles on the top and pressed with "stone", (f) S_{max} with PVC stripes on the top covered with rubber particles and pressed with the smooth stone.

Source: own.

If the coarsely ground rubber was uniformly sprinkled on the bottom of the mould, putting the highly viscous slurry over rubber particles changed their distribution into random, i.e., highly dependent on the moulding procedure (Figure 12 (c)). If the

pressure inflicted onto the casted slurry was too high, the slurry started escaping the mould next to the smooth stones placed on top of the slurry (placement of the stone is shown in Figure S1). Nonetheless, in this stage, it was still possible to correct the future pavement stone, i.e., the slurry was just put back into the mould, covered with PVC again, and with smooth stone that offered constant pressure onto the slurry.

To maintain a uniform distribution of the rubber particles over the entire surface, it was necessary to sprinkle coarsely ground rubber on top of the formed and already moulded slurry precisely and evenly (the procedure is shown in the Supplement in Figure S1). While the amount of rubber used in the S_{min} sample was fully integrated into the pavement stone (Figure 12 (e)), the amount of rubber used in S_{max} was exceeded. From the difference between used and fallen-off rubber, the amount of the integrated rubber into the slurry while being pressed by 0.76 kPa is approximately 0.11 g/cm^2.

To evaluate the hypothesis behind this work that the *addition of the coarsely ground rubber onto the surfaces of alkali-activated pavement stones enhances walking safety*, slipperiness was evaluated on not curved pavement stones in dry and wet conditions and is presented in Table 5. The lower the angle of the measurement, the lower the friction and the higher the slipperiness. Taking into account, that the wet walking surface defined as slippery for areas with a higher frequency of users (hospitals, shopping centres) is 35°or lower, and for all other areas 25°, the alkali-activated MK without rubber (mixture MK_b) is highly slippery for all areas. However, the minimal addition of the coarsely ground rubber used in this work (S_{min}) is enough to consider the pavement stones to be non-slippery for areas with lower frequencies, but it is still not good enough for high-frequency areas. For those areas, the maximal addition of the rubber used (S_{max}) was satisfactory, especially if the rubber was placed with a pattern (stripes) and not uniformly all over the surface. The result in the wet conditions was similar for striped pavement stone when tested parallel or perpendicular to the stripes, i.e., 5 $S_{\%}$ (surface percentage) bigger rubber contact surface (more rough area) for pendulum sliding over pavement stone parallel to the stripes was an insignificant difference for the overall coefficient of the friction.

Worth taking into consideration is also that all the pavement stones prepared with the maximal amount of the coarsely ground rubber did not have perfectly smooth surfaces (hills and valleys), i.e., movement of the pendulum could have been additionally hindered by it and not solely by the addition of the rubber.

Table 5: Angle reached by a pendulum which slid over the surface of the pavement stone.

Sample	Angle [°]	
	Dry	**Wet**
MK_b	63.8	14.6
S_{min} rubber up	64.0	27.4
S_{max} rubber up	57.2	36.4
S_{max} rubber down and bigger force	67.8	57.8
S_{max} rubber up and striped – parallel	54.4	45.4
S_{max} rubber up and striped – perpendicular	68.6	45.6

8 Conclusions

The hypothesis that the coarsely ground waste rubber spread onto the surface of alkali-activated slurry can give to the alkali-activated material's surface enhancement in being non-slippery was proven in this preliminary work. However, the optimal amount of addition of the rubber particles should be evaluated in further work, as well as the most optimal pattern of the rubber on the pavement stone's surface, and forces that offer good encapsulation of the rubber and the highest possible friction in the wet conditions.

Besides that, coarsely ground waste rubber has a high potential to be used on the surface of alkali-activated materials if ignited at 550 °C or 950 °C. While showing a high hydroscopic effect, it could be used as a precursor in alkali activation and not just as a filler.

Acknowledgment

This work is part of the ARRS project of Barbara Horvat, Ph.D., and was financially supported by the Slovenian Research Agency under Grant No. J2-3035 and also by Slovenian Research Agency program group no. P2-0273.

References

Afshinnia, K., Poursaee, A., 2015. The influence of waste crumb rubber in reducing the alkali–silica reaction in mortar bars. Journal of Building Engineering 4, 231–236. https://doi.org/10.1016/j.jobe.2015.10.002

Češnovar, Traven, Horvat, Ducman, 2019. The Potential of Ladle Slag and Electric Arc Furnace Slag Use in Synthesizing Alkali Activated Materials; the Influence of Curing on Mechanical Properties. Materials 12, 1173. https://doi.org/10.3390/ma12071173

Coran, A.Y., 2013. Vulcanization, in: The Science and Technology of Rubber. Elsevier, pp. 337–381. https://doi.org/10.1016/B978-0-12-394584-6.00007-8

Flory, P.J., n.d. Molecular Theory of Rubber Elasticity. Polymer Journal 17, 1–12.

Horvat, B., Češnovar, M., Traven, K., Pavlin, M., König, K., Ducman, V., 2022a. Influence of Homogenization of Alkali-Activated Slurry on Mechanical Strength, in: 3rd International Conference on Technologies & Business Models for Circular Economy: Conference Proceedings. Presented at the International Conference on Technologies & Business Models for Circular Economy, University of Maribor Press, pp. 11–50. https://doi.org/10.18690/um.fkkt.2.2022.2

Horvat, B., Ducman, V., 2020. Influence of Particle Size on Compressive Strength of Alkali Activated Refractory Materials. Materials 13, 2227. https://doi.org/10.3390/ma13102227

Horvat, B., Ducman, V., 2019. Potential of Green Ceramics Waste for Alkali Activated Foams. Materials 30. https://doi.org/doi:10.3390/ma12213563

Horvat, B., Ducman, V., Pavlin, A.S., 2019a. Waste Foundry Sand as Precursor in Alkali Activation Process. Livarski vestnik 66, 13.

Horvat, B., Mušič, B., Pavlin, M., Ducman, V., 2023. Microwave Irradiation of Alkali-activated Metakaolin Slurry, in: 5th International Conference on Technologies & Business Models for Circular Economy: Conference Proceedings. Presented at the International Conference on Technologies & Business Models for Circular Economy, University of Maribor Press, pp. 9–24. https://doi.org/10.18690/um.fkkt.1.2023.2

Horvat, B., Mušič, B., Pavlin, M., Ducman, V., 2022b. Microwave irradiation of alkali-activated metakaolin slurry. Presented at the 5th International Conference on Technologies & Business Models for Circular Economy. https://doi.org/10.18690/um.fkkt.6.2022

Horvat, B., Pavlin, A.S., Ducman, V., 2019b. Foundry wastes as potential precursor in alkali activation technology, in: Technologies & Business Models for Circular Economy. Presented at the 2nd International Conference on Technologies & Business Models for Circular Economy, Univerzitetna založba Univerze v Mariboru/University of Maribor Press.

Horvat, B., Pavlin, M., Ducman, V., 2022c. Influence of microwaves in the early stage of alkali activation on the mechanical strength of alkali-activated materials. Ceramics International. https://doi.org/10.1016/j.ceramint.2022.12.133

Leong, S.-Y., Lee, S.-Y., Koh, T.-Y., Ang, D.T.-C., 2023. 4R of rubber waste management: current and outlook. J Mater Cycles Waste Manag 25, 37–51. https://doi.org/10.1007/s10163-022-01554-y

Miller, N., n.d. The industry creating a third of the world's waste [WWW Document]. URL https://www.bbc.com/future/article/20211215-the-buildings-made-from-rubbish (accessed 7.18.23).

Mutalib, N.A.N.A., Mokhatar, S.N., Budiea, A.M.A., Jaini, Z.M., Kamarudin, A.F., Noh, M.S.M., 2021. A review: Study on waste rubber as construction material. IOP Conf. Ser.: Mater. Sci. Eng. 1144, 012003. https://doi.org/10.1088/1757-899X/1144/1/012003

Nuzaimah, M., Sapuan, S.M., Nadlene, R., Jawaid, M., 2018. Recycling of waste rubber as fillers: A review. IOP Conf. Ser.: Mater. Sci. Eng. 368, 012016. https://doi.org/10.1088/1757-899X/368/1/012016

Pavlin, M., Horvat, B., Frankovič, A., Ducman, V., 2021. Mechanical, microstructural and mineralogical evaluation of alkali-activated waste glass and stone wool. Ceramics International S0272884221004168. https://doi.org/10.1016/j.ceramint.2021.02.068

Škvára, F., 2007. Alkali Activated Material - Geopolymer 16.

Supplement

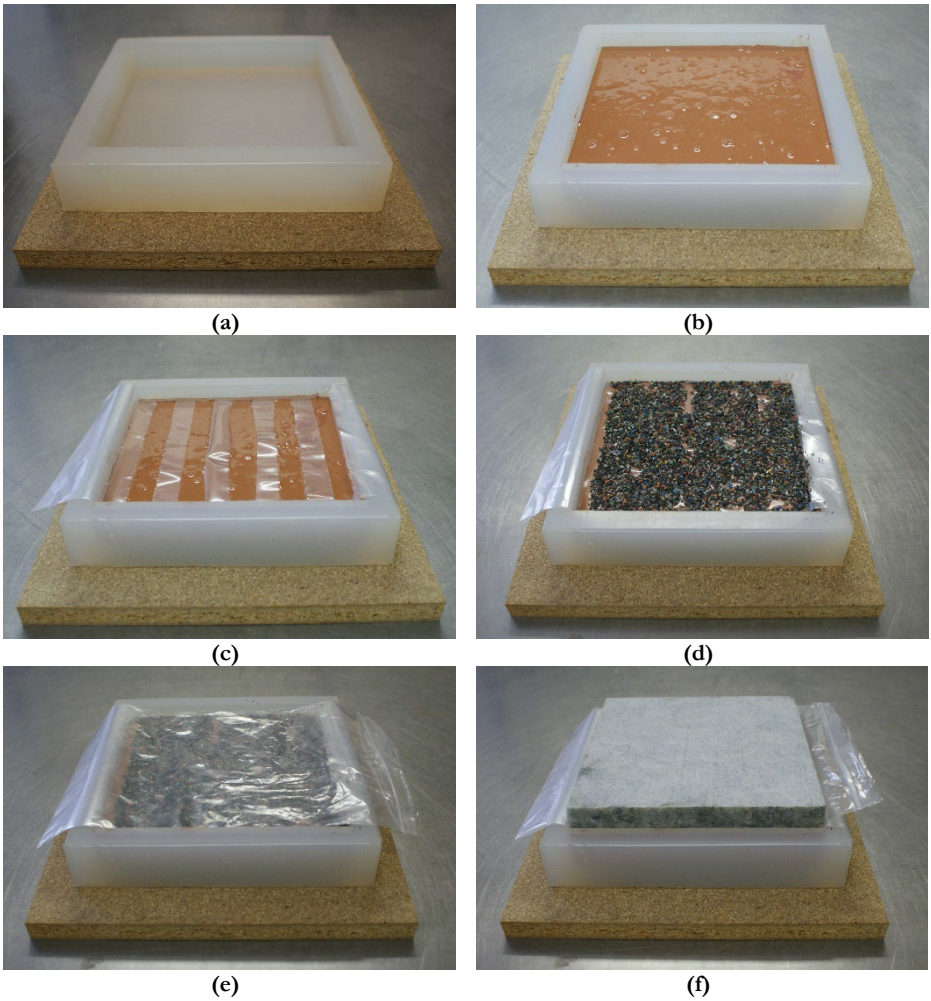

Figure S1: Pavement stone-making procedure.
Source: own.

EDXS areas of the acquisition of the signal from rubber are shown in Figure S2 and are labeled according to Table 3.

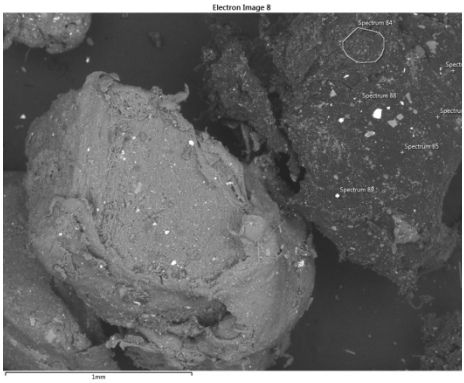

(b-dark grey)

(b-light grey)

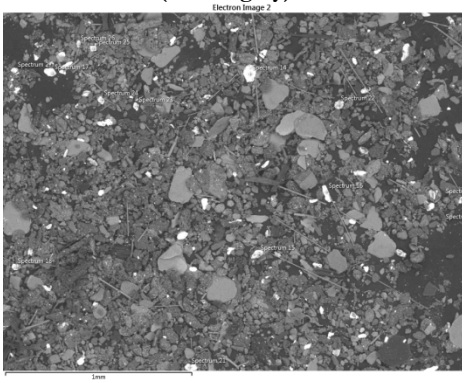

(c-white)

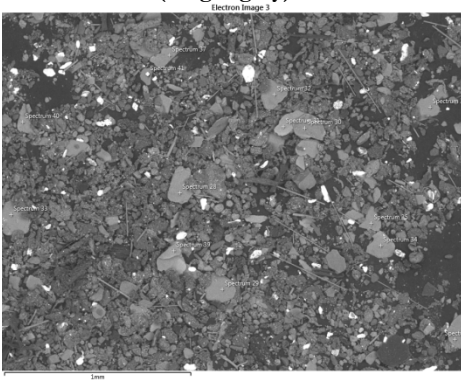

(c-light grey)

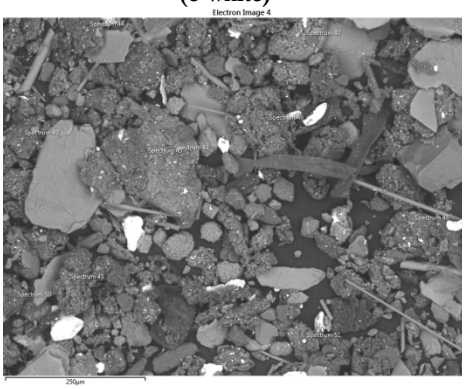

(c-middle grey random)

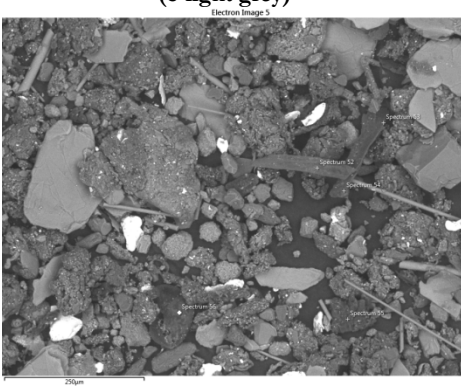

(c-dark grey leaves)

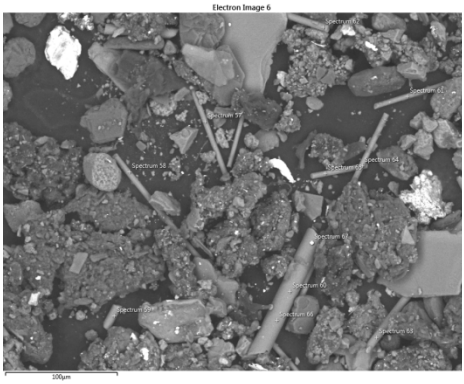

(c-middle grey fibres)

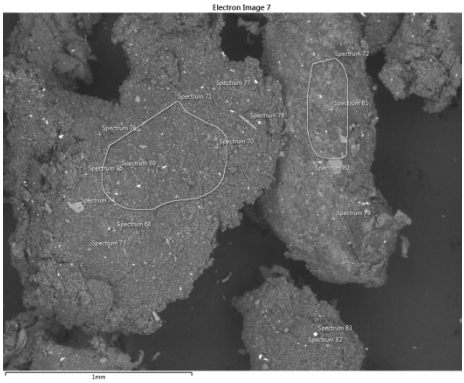

(c-middle grey)

(d-light grey/grey)

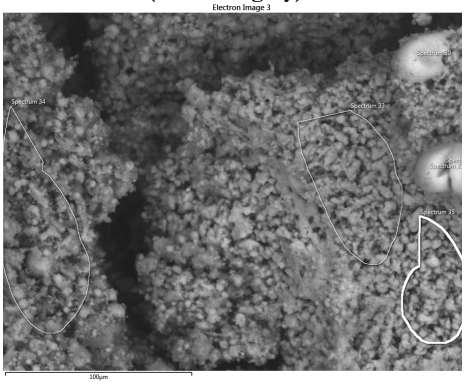

(d-light grey)

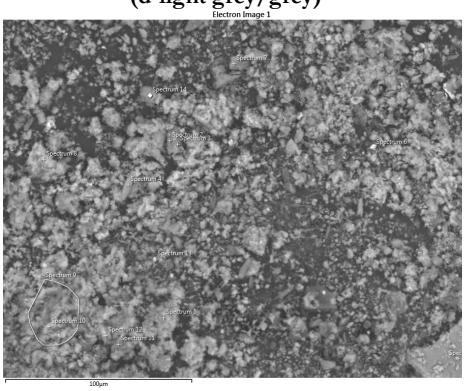

(e-light grey)

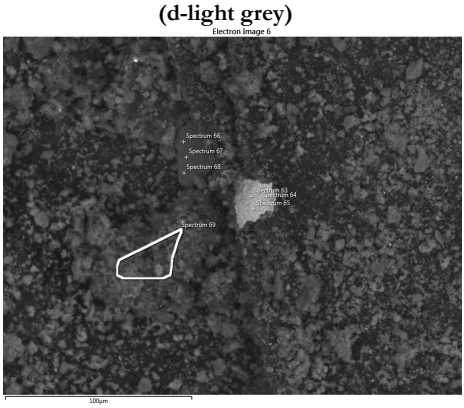

(e-white/middle grey/plates)

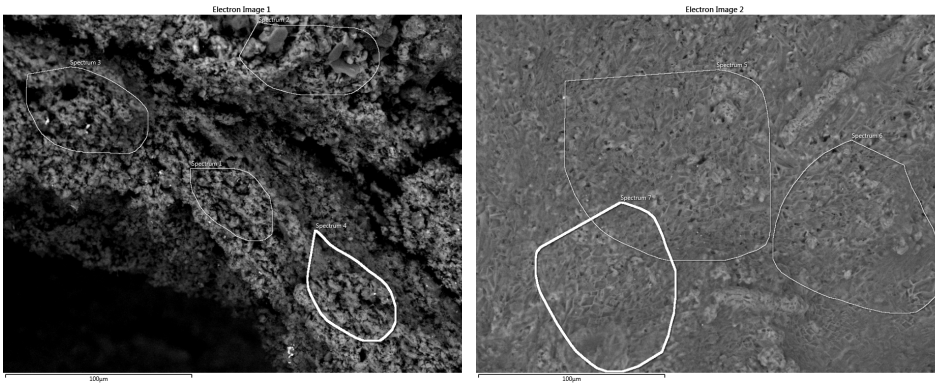

(f-grey) **(f-light grey)**

Figure S2. Locations of EDXS analysis performed on (b) coarse rubber and (a) fine rubber, and on rubber ignited at 550 °C (d) without and (e) with the gentle crushing of ignited rubber, and (f) ignited at 950 °C. Areas of the acquisition are labeled according to their greyscale and shape.

Source: own.

EDXS areas of the acquisition of the signal from ASN and rubber incorporated in the AAM are shown in Figure S3.

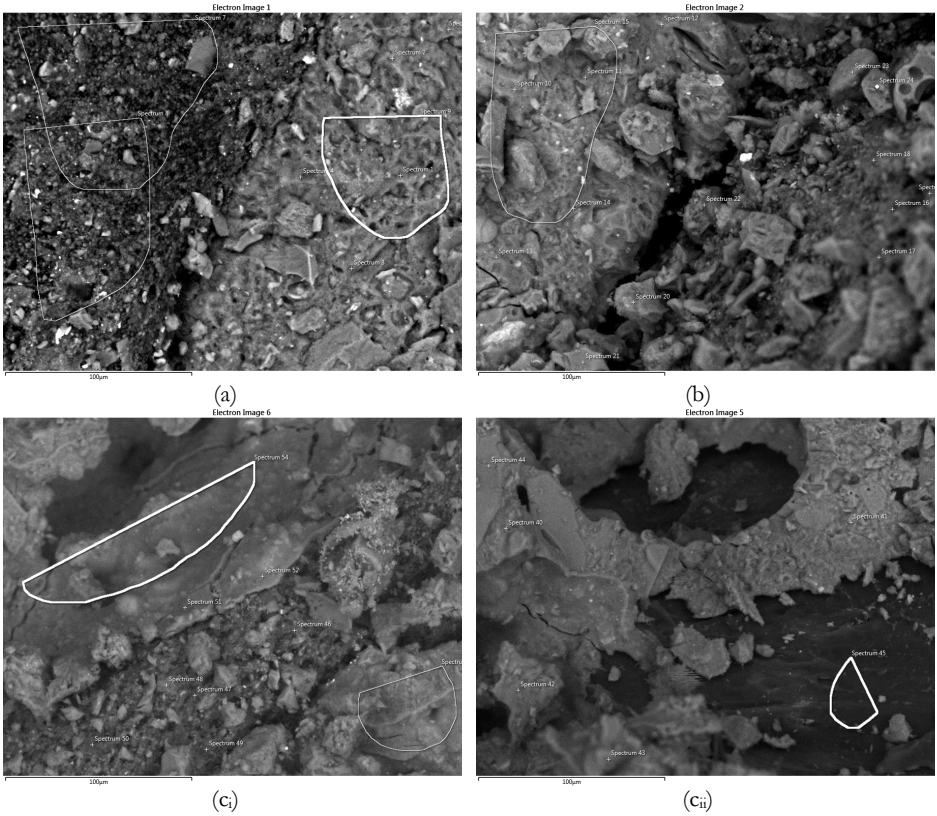

Figure S3: Locations of EDXS analysis performed on AAM cured (a) solely at room conditions, (b) at 100 W for 1 min, and (c_i, c_{ii}) at 1000 W for 1 min.
Source: own.